HHS Public Access

Author manuscript

Top Magn Reson Imaging. Author manuscript; available in PMC 2018 April 10.

Published in final edited form as:

Top Magn Reson Imaging. 2016 October ; 25(5): 215–221. doi:10.1097/RMR.0000000000000098.

Magnetic Resonance Imaging and Spectroscopy in Cancer Theranostic Imaging

Marie-France Penet[1,2], **Jiefu Jin**[1], **Zhihang Chen**[1], and **Zaver M. Bhujwalla**[1,2]

[1]JHU ICMIC Program, Division of Cancer Imaging Research, Russell H. Morgan Department of Radiology and Radiological Science, The Johns Hopkins University School of Medicine, Baltimore, MD

[2]Sidney Kimmel Comprehensive Cancer Center, The Johns Hopkins University School of Medicine, Baltimore, MD

Abstract

With its exquisite anatomical resolution and wide-ranging functional imaging capabilities, magnetic resonance imaging (MRI) has found multiple applications in detection, staging, and monitoring treatment response in cancer. The metabolic information provided by magnetic resonance spectroscopy (MRS) is being actively investigated to complement MRI parameters, as well as existing biomarkers, in cancer detection and in monitoring response to treatment. Located at the interface of detection and therapy, theranostic imaging is a rapidly expanding new field that is showing significant promise for precision medicine of cancer. Innovations in the development of novel nanoparticles decorated with imaging reporters that can be used to deliver therapeutic cargo to specific cells and environments have provided new roles for MRI and MRS in theranostic imaging.

Introduction

The recent emphasis on precision medicine strongly resonates in cancer treatment where conventional treatments can inflict significant collateral damage. Although significant inroads are being made with targeted treatments using antibodies against HER2[1] or epidermal growth factor receptor (EGFR)[2] or pharmacological agents that disrupt specific pathways (*e.g.*, PI3K/Akt[2-3] and mitogen-activated protein kinase (MAPK) inhibitors[4]), treatments that target only tumors with minimal impact on normal tissues continue to be an exception rather than the norm.

Tumors represent a complex ecosystem with cancer cells enmeshed in an extracellular matrix that contains stromal cells such as fibroblasts, immune cells, blood vessels, and endothelial cells[5] that are collectively termed the tumor microenvironment (TME). Components of the TME are frequently co-opted by cancer cells to survive, invade and form distant metastasis [6]. Abnormalities in vasculature, lymphatics, and metabolism create

*Correspondence to: Marie-France Penet, Ph.D. Division of Cancer Imaging Research, Department of Radiology, Johns Hopkins University School of Medicine, 212 Traylor Building, 720 Rutland Avenue, Baltimore, MD 21205, USA. Phone: 410-955-4220, Fax: 410-614-1948, mpenet@mri.jhu.edu.

heterogeneities in hypoxia, interstitial pressure and acidic microenvironments [7] that continually change, highlighting the importance of using noninvasive imaging to follow these dynamics [8]. Importantly, both cancer cells and the TME can be exploited for theranostic strategies [9] by incorporating imaging reporters within the carrier to detect the target of interest, and ascertain that the carrier with the therapeutic payload is at the target of interest and has cleared from normal tissue, before activating the therapy (schematic in Figure 1). Such imaging-based theranostic strategies provide tangible hope for cancer precision medicine. In addition, the functional imaging abilities of MRI and MRS [10] can be integrated into evaluating the response of the tumor to treatment.

Here we have presented examples of recent advances in the applications of MRI/S in cancer theranostic imaging strategies. These examples include non-targeted and targeted strategies, as well as strategies to specifically trigger the release of a drug within the tumor tissue. Examples are also provided to demonstrate the use of MRS and MRSI to evaluate treatment efficacy. These examples illustrate the increasing importance of MRI and MRS in theranostics that, with the ease of clinical translatability of MR techniques, are likely to find translation to human applications.

A. Non-targeted theranostic strategies

The increased permeability of tumor vasculature results in an enhanced permeability and retention (EPR) effect [11] that can be used to effectively deliver non-targeted nanoparticles of ~ 5-100 nm in size to tumors through prolonged circulation. Most nanoparticles used for theranostics typically fall within this range and achieve prolonged circulation by avoiding rapid renal and hepatic clearance.[12] Non-targeted passive EPR-based tumor delivery was demonstrated in a theranostic approach that combined the delivery of small interfering RNA (siRNA) with a prodrug enzyme.[13] The siRNA was directed against choline kinase, an enzyme overexpressed in cancer cells that phosphorylates free choline to phosphocholine. The pro-drug enzyme, bacterial cytosine deaminase (bCD), converted the non-toxic prodrug 5-fluorocytosine (5-FC) to cytotoxic 5-fluorouracil (5-FU). The nanoplex was labeled with gadolinium for MR imaging.[14] By combining both therapeutic approaches into a single treatment, selective targeting of cancer cells was amplified while minimizing damages to normal tissue. Quantitative T_1 imaging was used to detect tumor delivery of the nanoplex (Figures 2A-B) and normal tissue clearance to time 5-FC administration, and ^{1}H and ^{19}F MRS were used to detect choline kinase down-regulation through the decrease of total choline in ^{1}H MRSI and to measure the conversion of 5-FC into 5-FU in ^{19}F MR spectra. Combined siRNA-prodrug enzyme treatment achieved higher tumor growth delay compared to either treatment alone in an orthotopic triple negative MDA-MB-231 human breast cancer model. [13, 14]

More recently, self-assembled gemcitabine-gadolinium nanoparticles were evaluated in the MDA-MB-231 model.[15] These nanoparticles, formed by supramolecular assembly, combined the anticancer drug gemcitabine-5-monosphosphate for therapy with gadolinium for MR imaging. Efficient delivery of the particles was detected *in vivo* by MRI resulting in a significant reduction of tumor growth.[15] Tumor growth control improved with the nanoparticle compared to administration of gemcitabine-5-monosphosphate alone.

B. Targeted theranostic strategies

While the EPR effect can be successfully used to deliver particles to the tumor, it is a passive mechanism that may lead to a heterogeneous delivery and to accumulation of particles in other organs, especially at inflammatory sites that could induce side effects. Active targeting of nanoparticles to specific cancer cell surface markers can improve their delivery and retention within the tumor to additionally minimize toxicity in normal tissues. New therapies specifically targeted to cancer cell surface markers are being developed, with different types of targeting moieties, such as antibodies, receptor antagonists, or peptides.

1. Prostate specific membrane antigen—PSMA is a type II integral membrane protein that has abundant expression on the surface of prostate carcinomas, particularly in androgen-independent, advanced and metastatic disease [16], making it an attractive target to image prostate cancer. High-affinity, gadolinium-based PSMA-targeted MR contrast agents have recently been developed to detect PSMA with MRI.[17] Higher uptake of PSMA targeted particle was detected in PSMA overexpressing PC3-PIP human prostate cancer xenografts compared to isogenic low PSMA expressing PC3-Flu human prostate cancer xenografts, while there was no difference observed with non-targeted particle.[17] The PSMA targeting moiety has been used in separate studies in combination with the bCD-siRNA nanoplex described earlier to achieve PSMA specific delivery of siRNA or cDNA in combination with a prodrug enzyme *in vivo* [18] for theranostic imaging of prostate cancer. [18a]

2. Interleukin 1 receptor—The interleukin 1 (IL1) receptor has been utilized for reducing brain edema in a glioblastoma model. Since edema is one of the most common complications of malignant brain tumors, Shevtsov *et al.*, demonstrated the efficacy of combining recombinant IL1 receptor antagonist (IL- 1Ra) to superparamagnetic iron oxide (SPIO) nanoparticles (SPIONs) to image and target peritumoral brain edema.[19] In the study, IL-1Ra was conjugated to a superparamagnetic nanoparticle, to achieve tumor retention of the conjugate, without compromising its biologic activity, in the C6 glioma model. The particle was visualized from the negative contrast generated in the MR images, as shown in Figure 3. Retention of the magnetic nanoparticles was detected from hypointense zones in the RARE-T_2-weighted images and in the FLASH images, as indicated by the red arrows (Figure 3A). The treatment significantly increased life span in comparison to non-treated or corticosteroid treated animals (Figure 3B). The anti-edema effect induced by the treatment was quantified by measuring peritumoral edema using diffusion-weighted imaging. The apparent diffusion coefficient (ADC) maps identified the presence of peritumoral edema in the SPION-injected rat, that was not detected in the SPION IL1Ra injected animal (Figure 3C).[19] This study demonstrated the theranostic potential of SPION-IL1Ra particles to image and target peritumoral brain edema.

3. Insulin-like growth factor 1 receptor—Another potential cell surface receptor incorporated in theranostic strategies is insulin-like growth factor 1 receptor (IGFR1). Expressed by both cancer cells and stromal cells in pancreatic cancer, IGFR1 can be used to improve the delivery and retention of theranostic particles.[20] Zhou *et al.*, synthesized IGFR1 targeted-iron oxide nanoparticles (IONP) that are biocompatible, biodegradable, and characterized by a strong T_2 effect, visible in T_2 and T_2*-weighted MRI (Figures 4A-C).

The study was performed on patient derived pancreatic cancer xenografts (PDX) implanted in nude mice. For therapeutic purpose, the particles were loaded with doxorubicin (DOX). The purpose of targeting the particles to IGFR1 expressing cells was to limit DOX cardiotoxic effects by achieving cancer cell-specific delivery of DOX-loaded nanoparticles to avoid systemic toxicity. IGF1-IONP induced a stronger reduction of signal intensity in the tumor, compared to non-targeted IONP (Figures 4A-C). Moreover, the IGF1-IONP-DOX particles induced a greater reduction of tumor growth compared to the non-targeted IONP-DOX particles and DOX alone (Figure 4C-D). The study confirmed the potential of using MRI to evaluate targeted particles delivery and to assess the therapeutic efficacy through change in tumor size in these PDX models.[20]

4. Folic acid receptor—The folic acid receptor is a single-chain glycoprotein that is highly overexpressed by multiple malignant tumors, including ovarian cancer, and as a consequence has been exploited for specific targeting of cancer cells since most healthy tissues have low expression of this receptor.[21] Zhang *et al.*, developed a folic acid-targeted Fe_3O_4 nanoparticle that generated negative contrast in T_2-weighted MR images. The particles were tested in an intraperitoneal SK-OV-3 human ovarian cancer xenograft model. [21] The nanoparticles bound specifically *in vitro* to folic acid receptors overexpressing SK-OV-3 human ovarian cancer cells without inducing cytotoxicity. *In vivo*, localization of the particles in intraperitoneal SK-OV-3 ovarian cancer xenografts was observed. Tumor detection was improved by using folic acid-targeted Fe_3O_4 nanoparticles compared to the non-targeted particles. These nanoparticles have the potential to be used as multifunctional nanoprobes for the diagnosis and treatment of ovarian cancer.[21] In another study, Vu-Quang *et al.*, synthesized a PLGA-PEG-Folate nanoparticle loaded with DOX, ICG (indocyanine green) and PFOB (perfluorooctylbromide) for therapy, optical near infrared (NIR) imaging and ^{19}F MR imaging respectively, offering a platform for diagnosis and therapeutic applications.[22] The folate targeted particles showed higher optical and MR signals in a subcutaneous nasopharyngeal epidermal carcinoma (KB) human cancer xenograft implanted in nude BALB/c mice than the non-targeted particles. Their study highlighted the importance of multimodality imaging reporters by demonstrating that NIR imaging may be needed as a supplement to ^{19}F MRI for accurate diagnosis, due to the low signal to noise ratio obtained *in vivo*. The combination of the sensitivity of NIR imaging, the specificity of ^{19}F MRI and the anatomic resolution of ^{1}H MRI are a promising strategy for *in vivo* diagnosis that, with the inclusion of DOX, combines therapy with diagnosis.[22]

C. Triggered drug release

The unique physiological TME of tumors with regions of hypoxia and acidic extracellular pH (pHe) or high degradative enzyme activities provide opportunities to design nanoparticles that release their content only in these environments, or through controlled activation to minimize damage to normal tissues [9]. The release of the encapsulated drug can be triggered either by a physiological characteristic of the tumor, such as acidic pH_e, cleavage by an enzyme [23], or by some external source of activation, such as ultrasound or light, specifically directed towards the tumor tissue after delivery of the particle. Imaging can be used to confirm the localization of the particle in the tumor prior to drug delivery activation.

1. pH-responsive theranostic strategies—Due to poor perfusion and increased glycolytic activity, the TME is frequently characterized by an acidic pH_e.[24] This acidic pHe influences tumor progression and treatment outcome. As tumor-specific physiological characteristic, it can be used to specifically target drug delivery to the tumor tissue by synthesizing pH-responsive particles. Ma *et al.*, developed a magnetic polymer nanocarrier that is responsive to acidic pH, loaded with DOX, and targeted to the folate receptor-α. The theranostic particle was tested in a subcutaneous experimental model of gastric cancer.[25] The iron oxide present in the particle allowed for MR detection. The poly(β-aminoester)s used in the particle present weakly basic character due to their tertiary amines, they are water soluble below pH 6.5 and non-soluble at neutral pH in water. The release of DOX was improved in acidic environment compared to neutral condition where only a slow sustained diffusion was observed. By targeting folate receptor-α, a membrane-bound protein overexpressed in various malignant tumors, the chemotherapeutic efficacy was improved and side effects on normal tissues were avoided. The particles localized specifically in the tumor and were efficiently internalized in the tumor cells through folate receptor-mediated endocytosis.[25] Induction of apoptosis was observed both *in vitro* and *in vivo* with their particles, without causing side effects.

Another novel pH activated theranostic strategy was recently described by Wang *et al.*, for the acidic pH responsive delivery of artemisinin.[26] In these studies, dual therapy consisting of phototherapy in combination with the chemotherapy agent artemisinin was delivered with a dual metal-organic framework (d-MOF) nanoparticle that served as a T_1-T_2 MRI contrast agent and a fluorescent optical imaging agent. The inner core of the MOF nanoparticle served as a photothermal therapy agent that could be activated with NIR light once tumor delivery was established. The outer core was designed for pH-responsive degradation to release artemisinin. Careful *in vitro* and *in vivo* characterization of the MOF nanoparticle in HeLa cells and tumors demonstrated the feasibility of nanoparticle detection by T_1 and T_2-weighted MRI and optical imaging, and the feasibility of combined photothermal therapy and chemotherapy in tumors with significant reduction of tumor volume compared to single treatments.[26]

2. Light-triggered drug release—Photothermal and photodynamic therapies are used to damage cancer cells using laser irradiation to generate heat or free radicals respectively at the tumor site.[27] Photothermal agents convert light energy into heat, causing a rise of local temperature that consequently kills the cells in the area. Cao *et al.*, developed a new magnetic nanoparticle that combines, within one system, chemotherapy, photothermal therapy and MRI for detection. The particle combined gadolinium-chelated silica nanospheres, DOX, and ICG in a poly diallyldimethylammonium chloride coating (PDC).[27] This coating was used to avoid quick release of the drug from the particle. FDA-approved ICG absorbs NIR light (700-1000 nm) to generate heat and damage cells. The particles were visible on T_1-weighted images, as shown in MCF7 cells. *In vitro*, an accelerated release of DOX was demonstrated under acidic conditions, accompanied by a photothermal effect induced by laser irradiation that not only increased the release of DOX but also improved the therapeutic efficacy.[27] Future *in vivo* studies with this nanoparticle are required to confirm the promising potential of this strategy.

3. Pulsed low intensity non-focused US—The release of encapsulated drugs can be triggered by non-focused ultrasound (US), as shown by Rizzitelli *et al.*[28] In their study, liposomes were developed that, when triggered by pulsed low intensity non-focused US, generated the release of the antitumor drug DOX and MRI contrast.[28] Pulsed low intensity non-focused US are pulsed planar acoustic waves with intensity lower than 10 W/cm^2 and US frequencies ranging from 20 kHz to 1-3 MHz.[29] The release of DOX results from mechanical interaction between the acoustic waves and the particles. These nanocarriers were tested in a syngeneic breast tumor model, and the results showed that MRI was useful for both confirming the drug delivery and assessing the efficacy of the treatment. Tumor growth was delayed following treatment with the particle, and the tumor growth reduction was improved after exposure to pulsed low intensity non-focused US, compared to the group that received the particles without the pulsed low intensity non-focused US.[28] To further improve treatment efficacy, two sequential pulsed US treatments are applied.[29] The first releases the drug from the liposomes circulating in the tumor blood vessel, and the second increases the vessel permeability, facilitating the diffusion of the drug in the tumor stroma.[29] These modified liposomes were tested in a mammary carcinoma model in BALB/C mice using TS/A cells. MRI was used to measure the tumor growth and to assess the gadolinium-loaded liposome delivery. This strategy improved the delivery of the drug, visualized by an increased concentration of gadolinium, and led to a total tumor regression.[29]

D. MR spectroscopy as a complementary tool for theranostic imaging

Despite sensitivity limitations, MRS and MRSI can be useful additions in theranostic approaches for diagnosis, and to assess the efficacy of the therapy by informing on tumor metabolism.

1. MRS/MRSI for diagnosis—MRS biomarkers can be used to better characterize tumor tissue and define tumor margins more precisely, as shown by Cordova *et al.* [30] Metabolic MRS maps were co-registered with surgical planning MR images and imported into a neuronavigation system to guide tissue sampling in glioblastoma patients who received 5-aminolevulinic acid fluorescent-guided surgery (5-ALA FGS) (Figure 5). Figure 5A represents a MR anatomic image superimposed with total choline (Cho)/N-acetyl aspartate (NAA) ratio contours, shown as fold increase of the ratio compared to contralateral white matter. Immunohistochemistry staining of Sox2 (SRY(sex determining region Y)-box2) was used to assess tumor cell infiltration in the resected biopsy (Figure 5B). The study demonstrated that MRSI could complement conventional MRI to improve identification of tumor infiltration, and detect regions at high risk for recurrence.[30] MRS allowed the identification of tumor tissue preoperatively based on metabolic perturbations, while fluorescent-guided surgery provided confirmation of infiltrating cells to direct tissue resection intra-operatively (Figure 5C). The study showed that integrating MRSI into therapy planning and response assessment in glioma could potentially improve the current standard of care for patients with glioma.[30]

2. Therapeutic assessment efficacy—MRS and MRSI can play important roles in theranostic strategies. For instance, ^{19}F MRS was used to assess the activity of the prodrug enzyme bCD in the tumor after injection of the prodrug 5-FC, by following the conversion

of 5-FC to cytotoxic 5-FU non invasively (Figure 6A-B).[13-14,18a] ^{1}H MRS and MRSI can also be applied to assess treatment efficacy if the therapeutic target affects metabolites that can be measured by ^{1}H MRS. For example, total choline concentration can be measured *in vivo*, and by targeting the enzyme choline kinase with siRNA, the efficacy of siRNA-mediated downregulation of choline kinase can be assessed through its effect on decreasing total choline as shown in Figures 6C-D.[14, 18a]

E. Metastatic disease

One major goal of theranostics is to target metastatic disease, as treatment options are extremely limited. Wang *et al.*, recently developed a multiwalled carbon nanotubes coated with manganese oxide and PEG to diagnose and treat metastatic lymph nodes with T_1-weighted MRI and photothermal therapy respectively.[31] These theranostic particles consisted of a therapeutic component, provided by the multiwalled carbon nanotubes that absorb light in the NIR region and convert it to heat, and an imaging component, provided by manganese that generated T_1 contrast to allow MRI detection and guide the laser for photothermal therapy. In this study, A549 cancer cells were injected in the footpad of nude mice, inducing solid lesions in their popliteal fossa 2 months post injection. The study showed efficient treatment in sciatic and popliteal lymph nodes[31], and demonstrated the potential of this theranostic strategy to treat metastatic disease.

Conclusion

MRI and MRS imaging capabilities are rapidly expanding beyond traditional anatomical and functional imaging, into molecular and theranostic imaging. This expansion is built upon some of the most innovative strategies in nanoparticle composition and development, together with advances in instrumentation and multimodality imaging systems such as PET-MR scanners. The advantages and limitations of various nanomaterials are extensively reviewed by Gobbo *et al*[32]. The examples presented in the current review demonstrate the exciting potential of MRI and MRS based theranostics to achieve precision medicine in cancer. A major challenge for this field continues to be clinical translation. This will require a concerted effort to standardize nanoparticle synthesis and production to achieve safety and reproducibility under good manufacturing practice, to establish protocols for quantitative estimates of nanoparticle concentrations, and most importantly, to obtain support through federal agencies and industry for advancing the evaluation of nanoparticles in clinical trials.

Acknowledgments

Support from NIH P30CA006973, R01CA73850, R01CA82337, R01CA193365, R01CA136576, R01CA138515, R21CA198243, and The Tina's Wish Foundation is gratefully acknowledged. We gratefully acknowledge useful discussions with Professor Klaas Nicolay.

References

1. Henricks LM, Schellens JHM, Huitema ADR, Beijnen JH. The use of combinations of monoclonal antibodies in clinical oncology. Cancer Treat Rev. 2015; 41(10):859–867. [PubMed: 26547132]
2. Li X, Wu C, Chen N, Gu H, Yen A, Cao L, Wang E, Wang L. PI3K/Akt/mTOR signaling pathway and targeted therapy for glioblastoma. Oncotarget. 2016

3. Yang SX, Polley E, Lipkowitz S. New insights on PI3K/AKT pathway alterations and clinical outcomes in breast cancer. Cancer Treat Rev. 2016; 45:87–96. [PubMed: 26995633]

4. Cheng YB, Zhang GH, Li G. Targeting MAPK pathway in melanoma therapy. Cancer Metast Rev. 2013; 32(3-4):567–584.

5. Albini A, Magnani E, Noonan DM. The tumor microenvironment: biology of a complex cellular and tissue society. Q J Nucl Med Mol Imaging. 2010; 54(3):244–8. [PubMed: 20639811]

6. Quail DF, Joyce JA. Microenvironmental regulation of tumor progression and metastasis. Nature medicine. 2013; 19(11):1423–37.

7. Cairns R, Papandreou I, Denko N. Overcoming physiologic barriers to cancer treatment by molecularly targeting the tumor microenvironment. Mol Cancer Res. 2006; 4(2):61–70. [PubMed: 16513837]

8. Stasinopoulos I, Penet MF, Krishnamachary B, Bhujwalla ZM. Molecular and functional imaging of invasion and metastasis: windows into the metastatic cascade. Cancer biomarkers : section A of Disease markers. 2010; 7(4):173–88.

9. Stasinopoulos I, Penet MF, Chen Z, Kakkad S, Glunde K, Bhujwalla ZM. Exploiting the tumor microenvironment for theranostic imaging. NMR in biomedicine. 2011; 24(6):636–47. [PubMed: 21793072]

10. Glunde K, Pathak AP, Bhujwalla ZM. Molecular-functional imaging of cancer: to image and imagine. Trends Mol Med. 2007; 13(7):287–97. [PubMed: 17544849]

11. Maeda H. The enhanced permeability and retention (EPR) effect in tumor vasculature: the key role of tumor-selective macromolecular drug targeting. Adv Enzyme Regul. 2001; 41:189–207. [PubMed: 11384745]

12. Longmire M, Choyke PL, Kobayashi H. Clearance properties of nano-sized particles and molecules as imaging agents: considerations and caveats. Nanomedicine (Lond). 2008; 3(5):703–17. [PubMed: 18817471]

13. Li C, Penet MF, Winnard P Jr, Artemov D, Bhujwalla ZM. Image-guided enzyme/prodrug cancer therapy. Clinical cancer research : an official journal of the American Association for Cancer Research. 2008; 14(2):515–22. [PubMed: 18223227]

14. Li C, Penet MF, Wildes F, Takagi T, Chen Z, Winnard PT, Artemov D, Bhujwalla ZM. Nanoplex delivery of siRNA and prodrug enzyme for multimodality image-guided molecular pathway targeted cancer therapy. ACS Nano. 2010; 4(11):6707–16. [PubMed: 20958072]

15. Li L, Tong R, Li M, Kohane DS. Self-assembled gemcitabine-gadolinium nanoparticles for magnetic resonance imaging and cancer therapy. Acta Biomater. 2016; 33:34–9. [PubMed: 26826531]

16. (a) Schulke N, Varlamova OA, Donovan GP, Ma D, Gardner JP, Morrissey DM, Arrigale RR, Zhan C, Chodera AJ, Surowitz KG, Maddon PJ, Heston WD, Olson WC. The homodimer of prostate-specific membrane antigen is a functional target for cancer therapy. Proc Natl Acad Sci U S A. 2003; 100(22):12590–5. [PubMed: 14583590] (b) Huang X, Bennett M, Thorpe PE. Anti-tumor effects and lack of side effects in mice of an immunotoxin directed against human and mouse prostate-specific membrane antigen. The Prostate. 2004; 61(1):1–11. [PubMed: 15287089]

17. Banerjee SR, Ngen EJ, Rotz MW, Kakkad S, Lisok A, Pracitto R, Pullambhatla M, Chen Z, Shah T, Artemov D, Meade TJ, Bhujwalla ZM, Pomper MG. Synthesis and Evaluation of Gd(III) - Based Magnetic Resonance Contrast Agents for Molecular Imaging of Prostate-Specific Membrane Antigen. Angew Chem Int Ed Engl. 2015; 54(37):10778–82. [PubMed: 26212031]

18. (a) Chen Z, Penet MF, Nimmagadda S, Li C, Banerjee SR, Winnard PT Jr, Artemov D, Glunde K, Pomper MG, Bhujwalla ZM. PSMA-targeted theranostic nanoplex for prostate cancer therapy. ACS Nano. 2012; 6(9):7752–62. [PubMed: 22866897] (b) Chen Z, Penet MF, Krishnamachary B, Banerjee SR, Pomper MG, Bhujwalla ZM. PSMA-specific theranostic nanoplex for combination of TRAIL gene and 5-FC prodrug therapy of prostate cancer. Biomaterials. 2016; 80:57–67. [PubMed: 26706476]

19. Shevtsov MA, Nikolaev BP, Yakovleva LY, Dobrodumov AV, Zhakhov AV, Mikhrina AL, Pitkin E, Parr MA, Rolich VI, Simbircev AS, Ischenko AM. Recombinant interleukin-1 receptor antagonist conjugated to superparamagnetic iron oxide nanoparticles for theranostic targeting of experimental glioblastoma. Neoplasia. 2015; 17(1):32–42. [PubMed: 25622897]

20. Zhou H, Qian W, Uckun FM, Wang L, Wang YA, Chen H, Kooby D, Yu Q, Lipowska M, Staley CA, Mao H, Yang L. IGF1 Receptor Targeted Theranostic Nanoparticles for Targeted and Image-Guided Therapy of Pancreatic Cancer. ACS Nano. 2015; 9(8):7976–91. [PubMed: 26242412]

21. Zhang H, Li J, Hu Y, Shen M, Shi X, Zhang G. Folic acid-targeted iron oxide nanoparticles as contrast agents for magnetic resonance imaging of human ovarian cancer. J Ovarian Res. 2016; 9(1):19. [PubMed: 27025582]

22. Vu-Quang H, Vinding MS, Nielsen T, Ullisch MG, Nielsen NC, Kjems J. Theranostic tumor targeted nanoparticles combining drug delivery with dual near infrared and F magnetic resonance imaging modalities. Nanomedicine : nanotechnology, biology, and medicine. 2016

23. Qin SY, Feng J, Rong L, Jia HZ, Chen S, Liu XJ, Luo GF, Zhuo RX, Zhang XZ. Theranostic GO-based nanohybrid for tumor induced imaging and potential combinational tumor therapy. Small. 2014; 10(3):599–608. [PubMed: 24000121]

24. (a) Gillies RJ, Robey I, Gatenby RA. Causes and consequences of increased glucose metabolism of cancers. J Nucl Med. 2008; 49(2):24S–42S. [PubMed: 18523064] (b) Gillies RJ, Gatenby RA. Hypoxia and adaptive landscapes in the evolution of carcinogenesis. Cancer Metastasis Rev. 2007; 26(2):311–7. [PubMed: 17404691]

25. Ma H, Liu Y, Shi M, Shao X, Zhong W, Liao W, Xing MM. Theranostic, pH-Responsive, Doxorubicin-Loaded Nanoparticles Inducing Active Targeting and Apoptosis for Advanced Gastric Cancer. Biomacromolecules. 2015; 16(12):4022–31. [PubMed: 26477267]

26. Wang D, Zhou J, Chen R, Shi R, Zhao G, Xia G, Li R, Liu Z, Tian J, Wang H, Guo Z, Chen Q. Controllable synthesis of dual-MOFs nanostructures for pH-responsive artemisinin delivery, magnetic resonance and optical dual-model imaging-guided chemo/photothermal combinational cancer therapy. Biomaterials. 2016; 100:27–40. [PubMed: 27240160]

27. Cao M, Wang P, Kou Y, Wang J, Liu J, Li Y, Li J, Wang L, Chen C. Gadolinium(III)-Chelated Silica Nanospheres Integrating Chemotherapy and Photothermal Therapy for Cancer Treatment and Magnetic Resonance Imaging. ACS Appl Mater Interfaces. 2015; 7(45):25014–23. [PubMed: 26418578]

28. Rizzitelli S, Giustetto P, Cutrin JC, Delli Castelli D, Boffa C, Ruzza M, Menchise V, Molinari F, Aime S, Terreno E. Sonosensitive theranostic liposomes for preclinical in vivo MRI-guided visualization of doxorubicin release stimulated by pulsed low intensity non-focused ultrasound. J Control Release. 2015; 202:21–30. [PubMed: 25626083]

29. Rizzitelli S, Giustetto P, Faletto D, Delli Castelli D, Aime S, Terreno E. The release of Doxorubicin from liposomes monitored by MRI and triggered by a combination of US stimuli led to a complete tumor regression in a breast cancer mouse model. J Control Release. 2016; 230:57–63. [PubMed: 27049069]

30. Cordova JS, Shu HG, Liang Z, Gurbani SS, Cooper LA, Holder CA, Olson JJ, Kairdolf B, Schreibmann E, Neill SG, Hadjipanayis CG, Shim H. Whole-brain spectroscopic MRI biomarkers identify infiltrating margins in glioblastoma patients. Neuro-oncology. 2016

31. Wang S, Zhang Q, Yang P, Yu XR, Huang LY, Shen S, Cai SJ. Manganese Oxide-Coated Carbon Nanotubes As Dual-Modality Lymph Mapping Agents for Photothermal Therapy of Tumor Metastasis. ACS Appl Mater Interfaces. 2016; 8(6):3736–3743. [PubMed: 26653008]

32. Gobbo OL, Sjaastad K, Radomski MW, Volkov Y, Prina-Mello A. Magnetic Nanoparticles in Cancer Theranostics. Theranostics. 2015; 5(11):1249–63. [PubMed: 26379790]

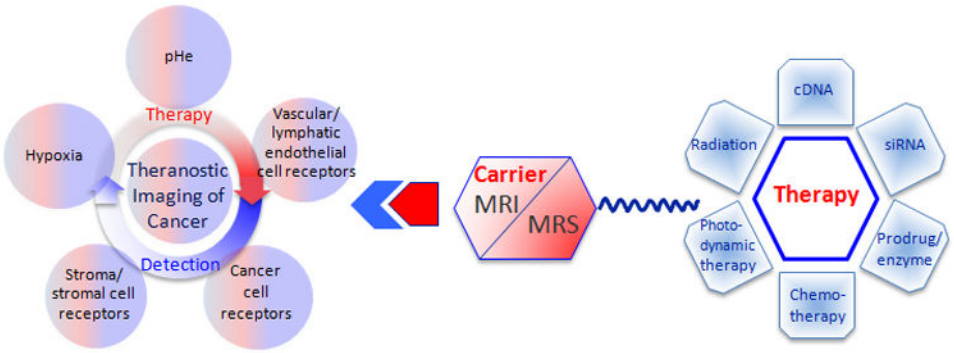

Figure 1.
Schematic representation of theranostic imaging.

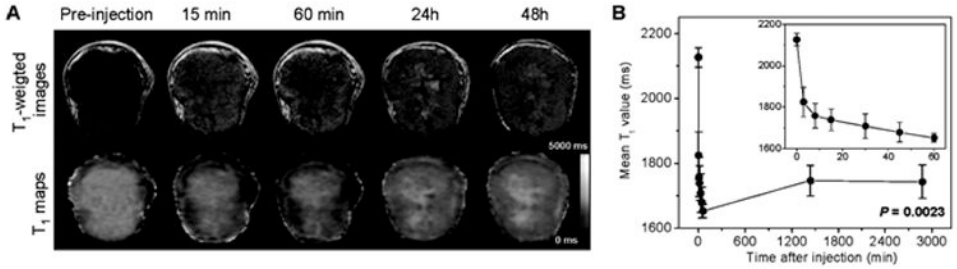

Figure 2.

(A) Representative *in vivo* T_1-weighted MR images (top panel) and quantitative T_1 maps (bottom panel) of a tumor pre- and post-injection of nanoplex (300 mg/kg, i.v.). (B) Time-dependent mean T_1 values of tumors pre- and post-injection of nanoplex; a significant decrease of T_1 ($P = 0.0023$) was observed up to 48 h. Inset panel shows the T_1 variation within the first 60 min of injection. Adapted with permission from [14]

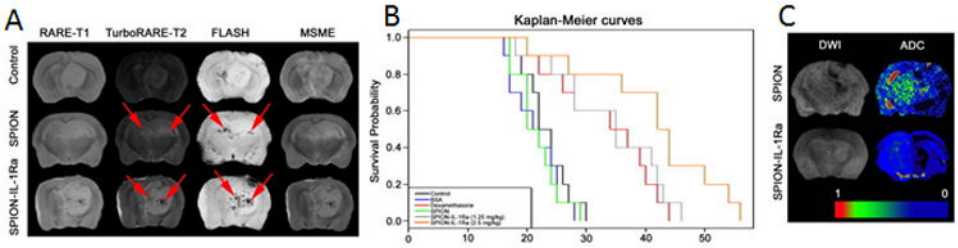

Figure 3.

C6 glioma targeting with SPION–IL-1Ra conjugates. (A) MRI of the C6 glioma 24 hours after i.v. injection of SPIONs or SPION–IL-1Ra conjugates. MR scans included RARE-T_1, TurboRARE-T_2, FLASH, and MSME sequences. (B) Kaplan-Meier survival curves for the control group and animals treated with BSA, dexamethasone, and SPION–IL-1Ra conjugates at 1.25 and 2.5 mg/kg of IL-1Ra. (C) DWIs and the corresponding ADC maps for the animals treated with SPION or SPION–IL-1Ra conjugates. Adapted with permission from [19]

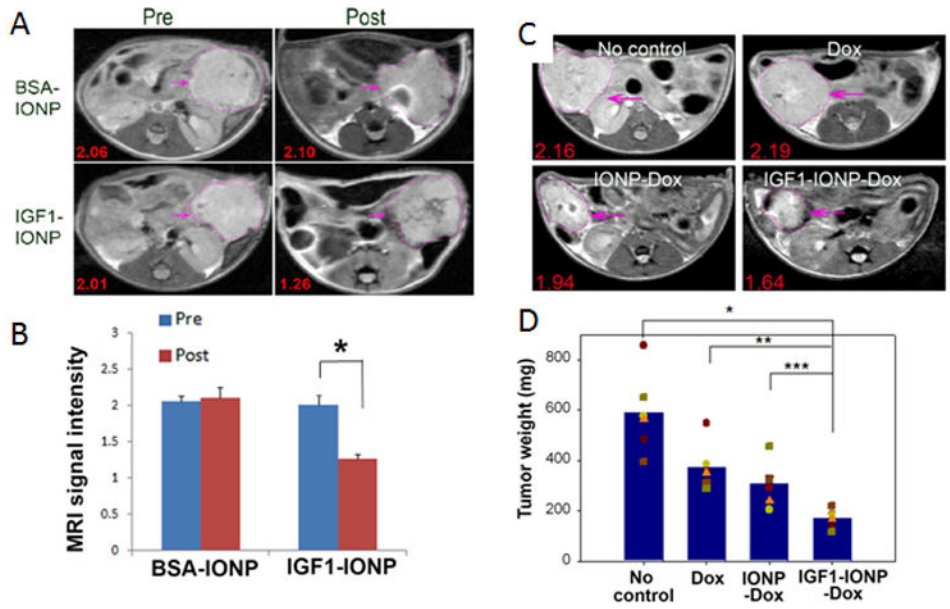

Figure 4.

Detection of targeted delivery of IGF1-IONPs by MRI and i*n vivo* antitumor effect in an orthotopic pancreatic PDX tumor model. (A) Pre and post injection T_2-weighted MR images with relative mean MRI signal intensities of the entire tumor. (B) Bar figure shows quantification of MRI signals in the tumor pre- and post injection of IONPs. Relative MRI signal was defined as the mean intensity of the tumor divided by the mean intensity of the muscle. $*p < 0.0001$. (C) T_2-weighted MRI of treated mice confirmed the accumulation of IGF1-IONP-Dox in the tumor and tumor growth inhibition compared to both free Dox- and non-targeted IONP-Dox-treated tumors. Red numbers show the mean of relative MRI signal intensities of MRI image slices from the entire tumor. A 10.2% MRI signal decrease was detected in non-targeted IONP-Dox-treated tumor, while a 24.1% MRI signal decrease was seen in IGF1-IONP-Dox-treated tumor. (D) Tumor growth inhibition. The mean tumor weight (navy bar) and individual tumor weight distributions as color symbols after the treatment are shown. $*p < 0.0001$; $**p < 0.0006$; $***p < 0.005$. Pink arrows indicate the location of pancreatic PDX-tumor lesions. Adapted with permission from [20].

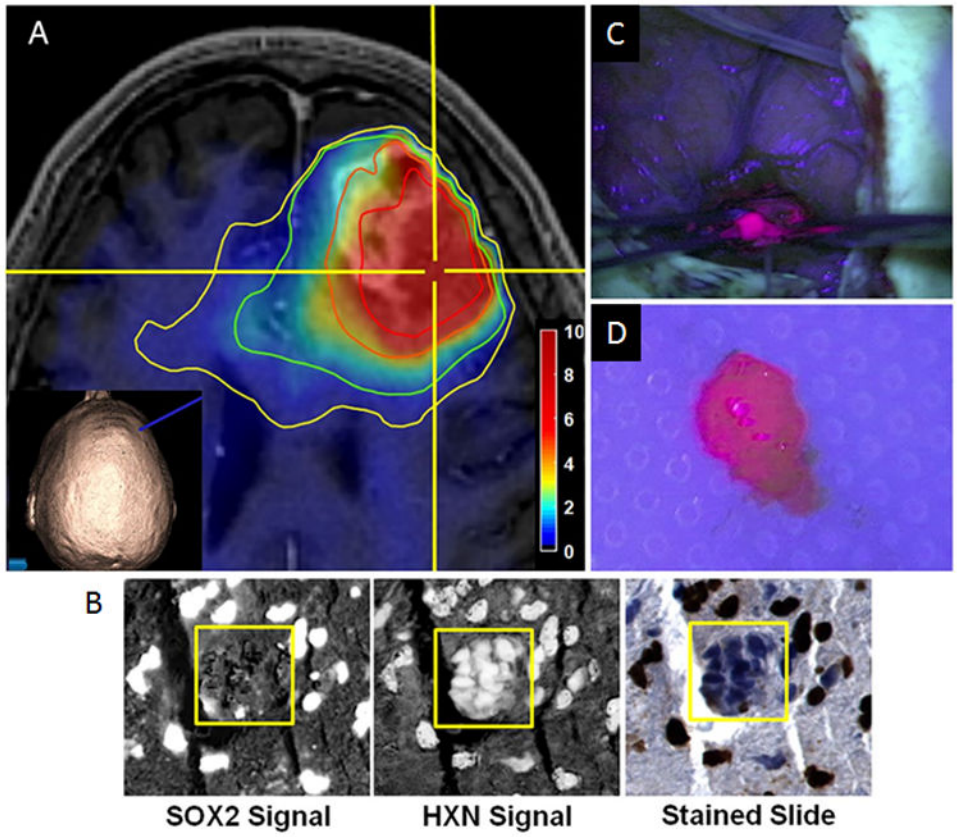

Figure 5.

Procedure for tissue sampling and histological analysis using MRSI and 5-ALA FGS. (A) View of anatomical and metabolic data in neuronavigation station with total choline(Cho)/N-acetyl-aspartate (NAA) ratio contours (yellow, 1.5-fold; green, 2-fold; orange, 5-fold; red, 10-fold increases in Cho/NAA over normal contralateral white matter). The inset image shows the 3D reconstruction of the patient surface anatomy along with the navigation probe (blue). Color bar depicts fold changes. (B) Automated nuclear segmentation, digital unmixing (pictured), and nuclear classification using machine-learning techniques allowed the generation of a Sox2 density metric that was correlated with MRSI and *ex vivo* fluorescence signal. (HXN, hematoxylin). (C) The region of metabolic abnormality was identified using a stereotactic technique with a location-reporting probe, and fluorescence was visualized using intraoperative microscopy. (D) Tissue was sampled in a biopsy-like fashion before debulking, and fluorescence was measured *ex vivo*. Adapted with permission from [30].

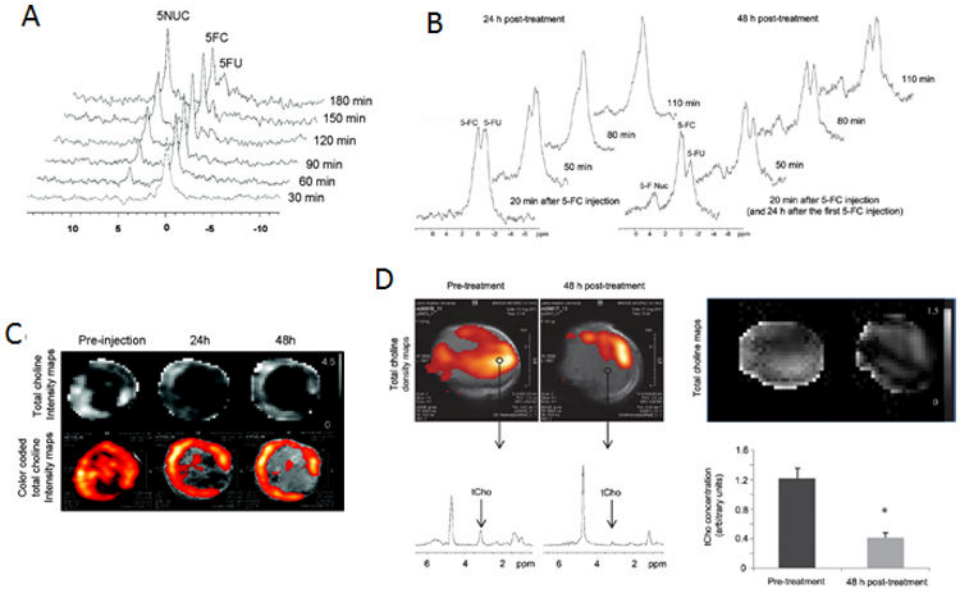

Figure 6.

(A) *In vivo* ^{19}F MRS demonstrated efficient conversion of prodrug 5-FC to 5-FU and its metabolites F-Nucl by nanoplex localized in MB-MDA-231 tumor. 5-FC was injected at 24 h after nanoplex injection. Adapted with permission from [14]. (B) *In vivo* ^{19}F MR spectra acquired from a PC3-PIP tumor at 24 and 48 h after i.v. injection of the PSMA-targeted nanoplex carrying bCD and siRNA-Chk. Spectra were acquired after a combined i.v. and i.p. injection of 5-FC.[18a] (C) Representative *in vivo* tCho maps and color-coded tCho intensity acquired in MB-MDA-231 tumor [14]. (D) *In vivo* tCho density maps from 2DCSI data sets acquired from a representative PC3-PIP tumor before and 48 h after i.v. injection of the PSMA-targeted nanoplex. Corresponding *in vivo* tCho maps from the same 2D CSI data sets. Representative one voxel spectra from the same 2D CSI (D) tCho concentration calculated in arbitrary units before and at 48 h after injection of the nanoplex. Adapted with permission from [18a].